

# Diesel exhaust-gas reforming for H<sub>2</sub> addition to an aftertreatment unit

A. Abu-Jrai<sup>a,1</sup>, A. Tsolakis<sup>a,\*</sup>, K. Theinnoi<sup>a</sup>, A. Megaritis<sup>b</sup>, S.E. Golunski<sup>c</sup>

<sup>a</sup> School of Engineering, Mechanical and Manufacturing Engineering, The University of Birmingham, Birmingham B15 2TT, UK

<sup>b</sup> Mechanical Engineering, School of Engineering and Design, Brunel University, West London, Uxbridge UB8 3PH, UK

<sup>c</sup> Johnson Matthey Technology Centre, Blount's Court, Sonning Common, Reading RG4 9NH, UK

Received 9 October 2007; received in revised form 19 December 2007; accepted 26 December 2007

## Abstract

The work described in this paper has been undertaken as part of the design of an integrated system comprising a diesel engine, an exhaust-gas fuel reformer and a NO<sub>x</sub> aftertreatment unit. The exhaust-gas reformer is used to provide hydrogen-rich reformat to the NO<sub>x</sub> aftertreatment unit, containing a hydrocarbon-SCR catalyst, in order to improve its NO<sub>x</sub> reduction activity at low exhaust-gas temperatures. The reformer configuration and operating parameters have been examined in order to optimise the performance of the hydrocarbon-SCR catalyst, which is promoted by the presence of H<sub>2</sub> but inhibited by CO. The length of the catalyst bed inside the reformer is a key factor in determining the extent to which the water-gas shift reaction can contribute to the reforming process, and therefore strongly influences the proportions of CO and H<sub>2</sub> in the reformat. However, it is also necessary for the reactant ratios at the reformer inlet to be controlled in response to changes in the engine operating conditions. In practice, this means that the rate of fuel addition to the reformer needs to be optimised for different exhaust gas compositions and space velocities. © 2008 Elsevier B.V. All rights reserved.

**Keywords:** Fuel reforming; Exhaust aftertreatment; Hydrocarbon-SCR; Hydrogen; Platinum catalyst

## 1. Introduction

The potential application of exhaust gas fuel reforming in internal combustion (IC) engines has been extensively studied, and the features that the reformer and catalyst design need to fulfil have been documented [1–3]. The technique involves reaction of fuel with engine exhaust gas (i.e. O<sub>2</sub>, H<sub>2</sub>O and CO<sub>2</sub>) in the presence of a catalyst to produce a gas that mainly contains H<sub>2</sub>, CO, H<sub>2</sub>O, CO<sub>2</sub> and N<sub>2</sub>. The reactor inlet feed ratios (O<sub>2</sub>/C and H<sub>2</sub>O/C) and the engine exhaust gas temperature are the main parameters that control the reactor product gas composition and operating temperature for a given reactor design (e.g. aspect ratio) [2,9]. The latest studies have significantly advanced reforming technology for automotive applications. For example, problems associated with start up of either the catalyst or the overall reformer and with flow control can now be resolved [10–12].

By incorporating a reformer in the EGR (exhaust gas recirculation) loop, the engine can be fed with reformed EGR (this is referred to as REGR), which has beneficial effects on both the engine performance and emissions [4–8]. The main challenge for the application of the REGR concept on-board a vehicle is the control of the reformer reactant flows (i.e. exhaust gas and fuel flows) under transient conditions (road conditions) in order to consistently provide the engine with optimum reactor product gas.

The addition of hydrogen-rich reformat to aftertreatment systems is also beneficial as it has been shown that hydrogen can improve the performance of catalytic aftertreatment devices in reducing emissions either directly [13–16] or by increasing the effectiveness of other agents in reducing emissions [17–20]. However, the demands made of a reformer in an REGR system [9] can be quite different from those required for promoting aftertreatment. As we have reported recently, the hydrocarbon-SCR activity window for a 1%Pt/Al<sub>2</sub>O<sub>3</sub> catalyst is shifted and also expanded towards lower inlet gas temperatures when H<sub>2</sub> is added in the gas feed [21]. However, the beneficial effects of H<sub>2</sub> can be seen only when there is a small concentration of CO (200 ppm) in the catalyst feed gas. Increased CO concentrations push the catalyst light-off to a higher temperature, where H<sub>2</sub> combustion predominates [22]. Consequently, it is evident that

\* Corresponding author. Tel.: +44 121 414 4170; fax: +44 121 414 7484.

E-mail addresses: ahmad\_abujrai@ahu.edu.jo (A. Abu-Jrai), a.tsolakis@bham.ac.uk (A. Tsolakis).

<sup>1</sup> Current address: College of Mining and Environmental Engineering, Al-Hussein Bin Talal University, Jordan. Tel.: +96232719000.

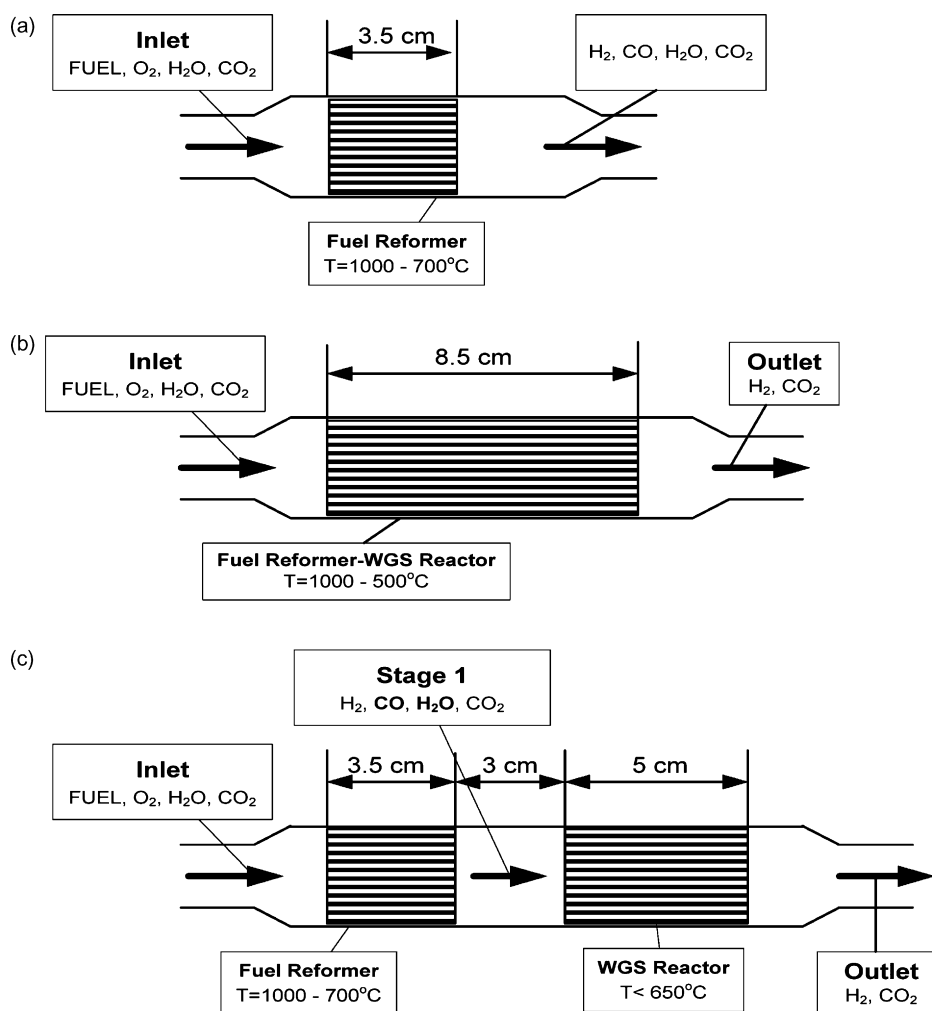
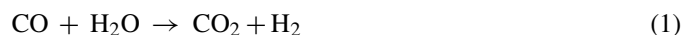


Fig. 1. Tested reformer configurations.

the incorporation of a reformer in the SCR system needs to be optimized in a way that the reformat CO content will be minimum while the H<sub>2</sub> content will be maximum. In addition, the reformer fuel efficiency will have to be as high as possible. The reaction that needs to be promoted is water gas shift (WGS), i.e. the reaction of CO with the available H<sub>2</sub>O to produce additional H<sub>2</sub> and CO<sub>2</sub>:



Despite the large number of publications related to fuel reforming and the effects of H<sub>2</sub> on the performance of exhaust-gas aftertreatment processes, there is not enough information regarding the reformer design requirements for optimum performance of the aftertreatment systems. In earlier work [21] we showed that it would not be appropriate to use partial oxidation to supply reformat to a hydrocarbon-SCR reactor containing a platinum catalyst, because of the relatively high CO/H<sub>2</sub> ratio in the reformat. In principle, autothermal reforming is more appropriate, but additional hardware would be required for the control of the reactants and for H<sub>2</sub> storage/supply under conditions where the activities of the reformer and the hydrocarbon-SCR reactor do not coincide. In REGR,

a small portion of the exhaust gas can be used as a source of the O<sub>2</sub>, H<sub>2</sub>O and CO<sub>2</sub> that reacts with injected fuel to produce a reformat that has a high H<sub>2</sub>/CO ratio [21]. The present study provides guidelines for optimisation of the REGR process, specifically as a means of supplying hydrogen-rich gas to a platinum hydrocarbon-SCR catalyst, in order to promote its low temperature NO<sub>x</sub> reduction activity.

## 2. Experimental

The experiments were carried out using actual engine exhaust gas from a Lister Petter TR1 diesel engine. The full engine test rig has been described in detail in previous publications [1,3]. The engine is an air-cooled, single-cylinder, direct injection diesel engine equipped with a Pump-Line-Nozzle (P-L-N) injection system. The main engine specifications are: bore 98.4 mm, stroke 101.6 mm, conrod length 165.0 mm, displacement volume 773 cm<sup>3</sup>, compression ratio 15.5, maximum power 8.6 kW at 2500 rpm and maximum torque 39.2 N m at 1800 rpm. The fuel used was ultra low sulphur diesel (average molecular formula: C<sub>15</sub>H<sub>28</sub>), which contained 24.4% aromatics and 35 mg kg<sup>-1</sup> sulphur and had a cetane number of 53.9.

Table 1  
Exhaust gas composition for the two tested engine operating conditions

	$\lambda = 4.25$	$\lambda = 3.25$
O <sub>2</sub> (%)	15.81	14.25
H <sub>2</sub> O (%) <sup>a</sup>	3.30	4.10
CO <sub>2</sub> (%)	3.30	4.30
CO (%)	0.016	0.01

<sup>a</sup> H<sub>2</sub>O contents are calculated values.

A reforming catalyst with a nominal composition of 1%Rh/CeO<sub>2</sub>-ZrO<sub>2</sub> (by weight) was used. It was a Johnson Matthey proprietary formulation designed to promote all the desired reactions (oxidation, steam reforming, WGSR), while at the same time inhibiting coke formation. The catalyst was made into an aqueous suspension, which was uniformly coated onto ceramic monolith substrates with a high cell density (900 cpsi).

The reforming tests were carried out using three different monolith configurations shown schematically in Fig. 1. All the monoliths had a diameter of 15 mm but their lengths were different. The monolith configuration shown in Fig. 1c was divided in two parts. In the first part the exothermic (e.g. combustion of part of the fuel) and endothermic reactions (e.g. steam and dry reforming) occurred and there was production of H<sub>2</sub> and CO at temperatures higher than 700 °C. The second monolith part was positioned at a distance of 3 cm downstream of the first part where the temperature was lower, in the range of 500–700 °C, and the WGSR was promoted. In all cases, the reformer was placed in a tubular furnace to mimic the engine exhaust gas temperature conditions, and temperature profiles were obtained by slowly withdrawing a fine thermocouple along the length of a central monolith channel. The reformer fuel injector was positioned 10 cm upstream of the catalyst, allowing the fuel to vaporize and mix with the exhaust gas before reaching the front face of the monolith.

Analysis of the exhaust gas and the reformer product gas stream included continuous measurement of carbon dioxide, carbon monoxide (both by non-dispersive infrared, NDIR), total hydrocarbons (flame ionization detector, FID), oxygen (electrochemical method) and NO<sub>x</sub> (chemiluminescence) emissions. The hydrogen and methane reformat concentrations were measured by gas chromatography.

In order to optimize the exhaust gas reactor feed ratios (O/C, O<sub>2</sub>/C and H<sub>2</sub>O/C) to achieve maximum H<sub>2</sub> production for dif-

ferent engine exhaust gas compositions, calculations based on the exhaust-gas oxygen, water, CO<sub>2</sub> and CO contents were carried out using the STANJAN equilibrium model (v 3.89, Stanford University). The concentrations of the minor exhaust-gas components, such as NO<sub>x</sub> and unburnt hydrocarbons, were not included in the equilibrium calculations. Thus, some of the differences between actual and calculated reformat compositions can be attributed to the kinetic effects of the minor species. The calculations were performed at constant pressure and temperature.

The effects of the O/C ratio on the reaction profiles were examined at two different engine operating conditions, i.e. two different exhaust gas compositions. The engine was operated at excess air ratios of  $\lambda = 3.25$  and  $\lambda = 4.25$  and the corresponding exhaust gas compositions are shown in Table 1.

### 3. Results and discussion

#### 3.1. Temperature profiles

All the temperature profiles recorded from the diesel fuel reforming experimental tests using the 3.5 and 8.5 cm long monoliths (Fig. 1a and b, respectively) at different O/C ratios for  $\lambda = 4.25$  are shown in Fig. 2. The temperature rose steeply and reached a peak value close to the inlet face of the catalyst bed before declining much more gradually. The onset of this peak was associated with a rapid decline in gas phase oxygen, indicating that the diesel fuel was oxidising as soon as it came into contact with the catalyst. Some of the generated heat was back-radiated, so that the gas temperature in the 1 cm preceding the catalyst bed was often 500–600 °C higher than the gas feed temperature of 300 °C.

The height of the temperature peak responded to changes in the gas feed (O/C ratio). With increasing O/C ratio, the maximum temperature rose, but it did not have a significant affect on the outlet temperature. As shown in Fig. 2a the last 1 cm of the 3.5 cm long monolith was still at a temperature in the range of 550–700 °C, which is favourable for the promotion of the WGSR. In the case of the 8.5 cm long monolith, more than half of its length (approx. 5 cm) was in this temperature range (Fig. 2b).

As it has been reported in an earlier publication, the height, width and position of the temperature peak responded to changes in the gas feed flow rate [9]. With increasing space velocity, the

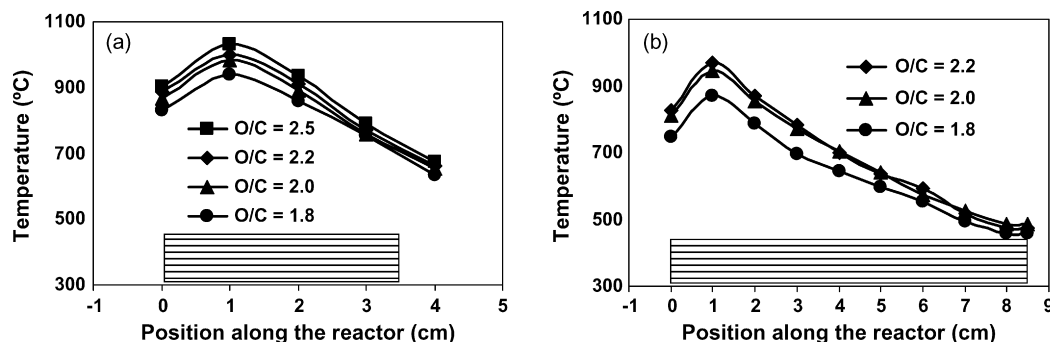


Fig. 2. Temperature profiles for (a) 3.5 cm and (b) 8.5 cm monoliths.  $\lambda = 4.25$ .

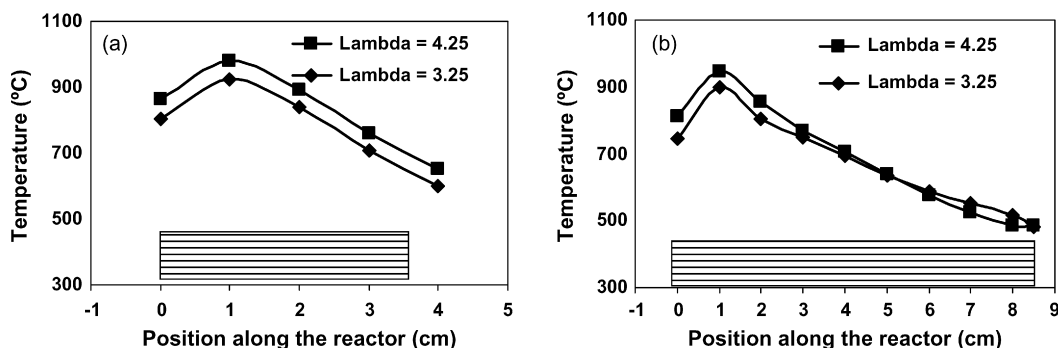


Fig. 3. Temperature profiles for (a) 3.5 cm and (b) 8.5 cm monoliths. O/C=2.0.

maximum temperature increased, the temperature peak shifted further downstream the catalyst bed and at the same time the temperature of the gases leaving the reactor was also increased.

Fig. 3a and b shows the temperature profiles recorded from the reforming of diesel fuel with an O/C ratio of 2 using the 3.5 and 8.5 cm monoliths, respectively. The O/C=2.0 ratio was kept constant by adjusting the fuel flow rate for each of the exhaust gas compositions that were obtained at the two different engine operating conditions of  $\lambda = 3.25$  and  $\lambda = 4.25$ . For both monolith configurations, the reactor temperatures were lower in the case where exhaust gas from the engine operating at the higher load (i.e.  $\lambda = 3.25$ ) was used. This is due to the higher H<sub>2</sub>O and lower O<sub>2</sub> content of the engine exhaust gas in this case compared to the lower load operating condition (i.e.  $\lambda = 4.25$ ).

In the case of the higher load operation more of the O atoms taken into account in the calculation of the O/C ratio were O atoms contained in the steam and less in the gas O<sub>2</sub> compared to the low load condition. In order to keep the O/C ratio the same under both high and low load engine operating conditions less fuel was required in the case of the higher load compared to the lower load operation (the exhaust gas flow into the reformer was kept the same under both operating conditions). The effects of the engine exhaust gas composition at different engine operating conditions on the reformer performance and product gas composition have been presented and discussed in detail in an earlier study [5].

### 3.2. Exhaust gas reforming – equilibrium calculations

The main reactions that take place in an exhaust gas reformer that contains a precious metal catalyst with composition similar to the one used in this study are oxidation, steam reforming (SRR), dry reforming (DRR) and water gas shift (WGS) irrespective of the fuel type or the configuration of the catalyst bed. This was a key outcome from our earlier work [2,9,23] but also from more recent work on partial oxidation by Horn et al. [24–26]. However, because these reactions occur consecutively at different stages of the catalyst bed, each providing new reactants and conditions downstream, the reaction rates of each reaction are affected differently by the monolith configuration (as well as the fuel type) [2]. Although the exothermic oxidation reactions generate heat close to the inlet face of the monolith, the onset of the endothermic H<sub>2</sub>-generating reactions

(e.g. SRR, DRR) reverses the temperature rise, resulting in a characteristic asymmetric-peak profile along the length of the reactor as shown in Fig. 4 (typical temperature profile based on the various recorded temperature profiles at different reactor conditions). In the cooler zone of the reactor, the WGSR and CO-methanation reaction become thermodynamically favoured. The catalyst is active for both these reactions, and the extent of their contributions can be determined by the position and size of the temperature peak in the catalyst bed [9].

As mentioned earlier, in the case where an exhaust gas fuel reformer will be incorporated into the engine exhaust to provide H<sub>2</sub>-rich gas to the SCR catalyst, an optimisation of the reactant feed rates will be required for the different engine exhaust gas compositions in order to increase H<sub>2</sub> production and eliminate CO. The amount of H<sub>2</sub>O at the inlet of the exhaust gas-reforming reactor is determined by the engine operating condition (i.e. air/fuel ratio). At the reactor inlet (high temperature zone), there is further H<sub>2</sub>O production due to the combustion of part of the feed fuel that is associated with the observed increase of the reactor temperature close to the inlet phase of the catalyst. Although part of the produced steam is used in the endothermic SRR, the remaining steam is available to be used in the WGSR under appropriate catalyst and reactor design conditions.

The ceria-supported rhodium catalyst is a recognised water gas shift catalyst under exhaust gas conditions [27]. Its optimum activity is restricted to a narrow range that is limited at low temperature by low turnover frequency and at high temperature by the predominance of the more thermodynamically favoured

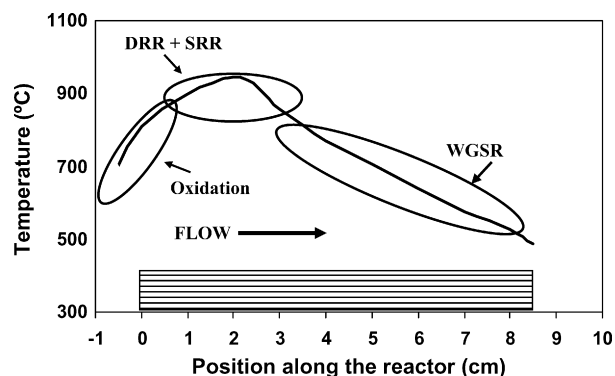


Fig. 4. Typical monolith temperature profile from the exhaust gas reforming at engine exhaust gas temperatures of around 300 °C.

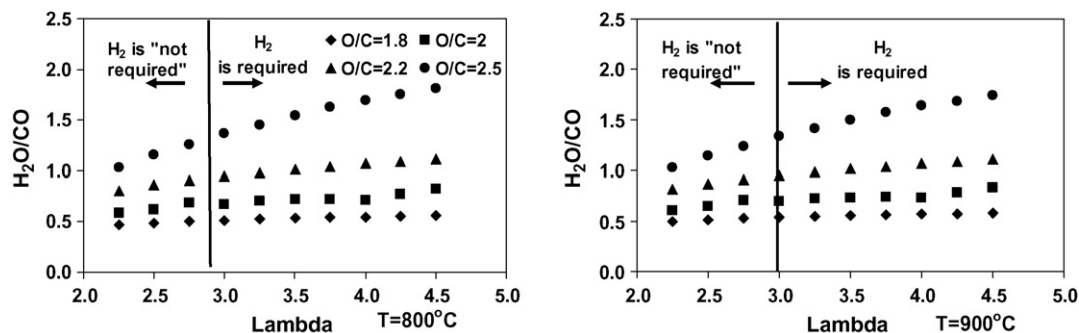


Fig. 5.  $H_2O/CO$  ratios for different engine operating conditions (different  $\lambda$ ) and O/C ratios. Reformer peak temperatures:  $T=800^\circ C$  (left graph) and  $T=900^\circ C$  (right graph).

reverse-shift reaction [28]. In earlier studies it has been estimated that the optimum water gas shift range of the present catalyst is  $550\text{--}700^\circ C$  [9]. For the monolith configuration shown in Fig. 1a, the promotion of the WGSR to consume the CO will require a catalyst capable of promoting this reaction at high temperatures. The catalyst configuration shown in Fig. 1b can promote the water-gas shift reaction better since with this configuration there is a presence of CO and  $H_2O$  at the part of the catalyst that is at temperatures below  $700^\circ C$ . The design shown in Fig. 1c is the most appropriate in terms of promoting the WGSR using the present catalyst composition. The second part of the monolith in this configuration can be positioned in an area where the temperature will always be in the range of  $550\text{--}700^\circ C$ .

In the cases of all the three monolith configurations a  $H_2O/CO$  molar ratio higher than 1 ( $H_2O/CO \geq 1$ ) is theoretically required in order to achieve consumption of the entire CO at the point where all the endothermic reactions have already occurred (i.e. complete use of diesel fuel) and there is not any further significant CO production or  $H_2O$  consumption (i.e. no further steam or dry reforming) [2,9]. From the temperature profiles shown in Figs. 2–4 and in agreement with earlier work where the same catalyst was used [2], this point is located in the area that is just downstream of the peak temperature point (approx. 2 cm downstream) and has a temperature lower than  $700^\circ C$ . The equilibrium programme is able to predict the product composition at the peak temperature but not the reactions occurring downstream of that point [9]. On this basis, the equilibrium program was used to identify the reactor feed ratios that would provide an  $H_2O/CO$  ratio of 1 at the peak temperature point. This is the optimum ratio that theoretically will result in the full CO consumption due to the promotion of the WGSR (Eq. (1)) downstream of that point with the best reforming process efficiency.

Fig. 5 shows the  $H_2O/CO$  ratio at the peak temperature point calculated using the equilibrium programme for different engine operating conditions (different  $\lambda$ ) and O/C ratios (1.8, 2, 2.2, 2.5). The maximum reaction temperature did not affect significantly the maximum produced  $H_2$  and, hence, results are presented only for the peak temperatures of 800 and  $900^\circ C$  although calculations were also carried out for 600 and  $700^\circ C$ .

As has been shown previously [21], the beneficial effects of hydrogen in improving the  $1\%Pt/Al_2O_3$  SCR catalyst performance in reducing  $NO_x$  are only seen at engine conditions where the exhaust gas temperatures are low ( $<230^\circ C$  approx.).

At higher exhaust gas temperatures the presence of  $H_2$  has no beneficial effects on the performance of the  $1\%Pt/Al_2O_3$  catalyst as at these conditions the  $NO_x$  emissions are reduced effectively through the hydrocarbon-SCR process. Thus, the  $H_2$  will be beneficial for the  $1\%Pt/Al_2O_3$  SCR catalyst at low engine load operation, i.e. low exhaust gas temperatures and high  $\lambda$ . For the engine used in this study, the reformer will not be required to provide reformat to the SCR catalyst at engine operating conditions with  $\lambda$  lower than approx. 3, where the exhaust gas temperatures are higher than  $250^\circ C$ .

As indicated in Fig. 5, in order to achieve the optimum  $H_2O/CO$  molar ratio of 1 at the peak temperature point, an O/C ratio of around 2.2 is required at the fuel reformer inlet independently of the peak temperature. The use of O/C ratios higher than 2.2 will result in the reduction of both the  $H_2$  production and the process efficiency. O/C ratios lower than 2.2 will result in increased  $H_2$  production and process efficiency but at the same time there will be a considerable CO production. The latter is undesirable since, as already mentioned, the beneficial effects of  $H_2$  on the SCR catalyst  $NO_x$  reduction activity are eliminated by CO.

Fig. 6 shows the maximum  $H_2$  production calculated at different temperatures mimicking peak catalyst bed temperatures for O/C = 2.2. In all cases the  $H_2$  production is in the range of 5–8%. However, the maximum theoretical  $H_2$  that can be produced at the outlet of the reactor by promoting the WGSR is the same for all temperatures (i.e. 600, 700, 800, and  $900^\circ C$ ) used in these calculations.

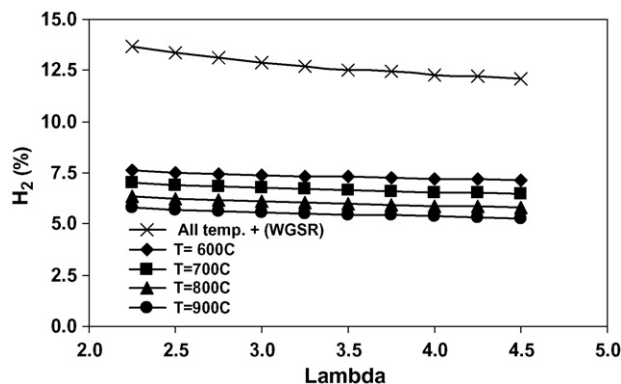
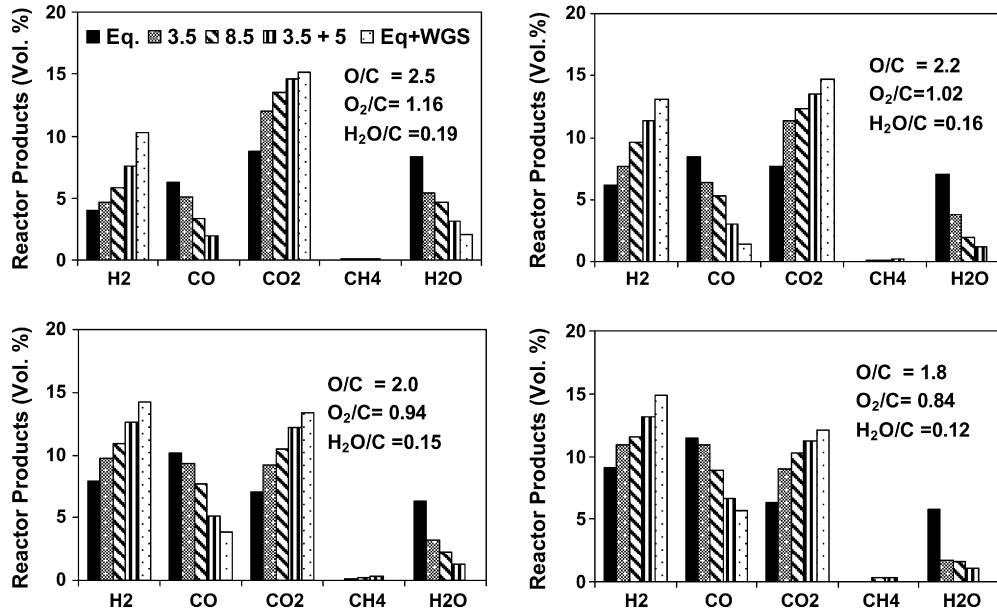


Fig. 6. Calculated hydrogen production with and without the contribution of the WGS reaction. O/C = 2.2.

Fig. 7. Reactor product gas composition for  $\lambda = 4.25$ .

### 3.3. Product distribution

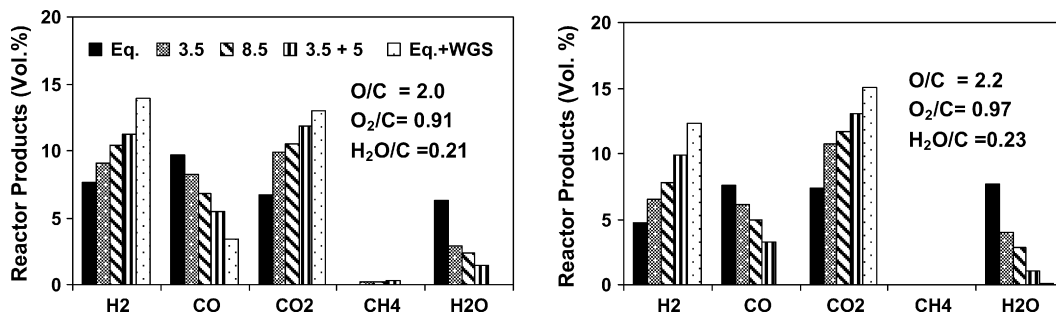
The measured and calculated product gas compositions at the outlet of the three tested reactor configurations (Fig. 1) are illustrated in Figs. 7 and 8 for different reactant ratios. The three monolith configurations are indicated in these figures by their respective lengths of 3.5, 8.5 and 3.5 + 5 cm. The calculated product gas compositions at the peak temperature with and without including the WGSR are also presented. The results indicated as 'Eq.' were obtained from the equilibrium calculations, while the results noted as 'Eq. + WGS' were obtained from the equilibrium calculations assuming that the whole  $\text{H}_2\text{O}$  calculated at the peak temperature point reacted with CO (WGSR) and additional  $\text{H}_2$  and  $\text{CO}_2$  were produced. This is the maximum  $\text{H}_2$  that would be produced with the used feed ratios with optimum catalyst and reactor design.

The actual reactor product gas composition in the case of the 3.5 cm long monolith (Fig. 1a) was the closest to the calculated equilibrium values ('Eq.'). The below-equilibrium CO and above-equilibrium  $\text{H}_2$  and  $\text{CO}_2$  concentrations in this case indicate that there was a small contribution from the WGSR, which took place in the cooler zone ( $<700^\circ\text{C}$ ) of the catalyst bed. Under these conditions, with the peak temperature of around

$900^\circ\text{C}$  (1 cm downstream of the catalyst inlet face), the WGSR was constrained either kinetically by the low contact time in the cooler zone, or thermodynamically by the relatively high temperature throughout the bed ( $600^\circ\text{C}$  at the outlet). On the other hand, in the case of the longer monolith (Fig. 1b) or the catalyst consisting of two parts (Fig. 1c) to promote the WGSR, the actual reactor product gas composition was closer to the calculated maximum  $\text{H}_2$  production ('Eq. + WGS'), and there was a significant reduction of the CO content of the reformer product gas.

### 3.4. Further discussion – reformer design implications

The results presented in the previous sections have revealed the importance of the reforming catalyst configuration as well as the reactant ratios, when it comes to the optimisation of the reformat composition required to achieve maximum hydrocarbon-SCR performance. The implication of these findings is that apart from the reformer design, the reactant flows will have to be optimised for different engine operating conditions, i.e. different exhaust gas compositions. The design of an exhaust gas fuel reformer for dual use, to provide reformat simultaneously to an engine and to an aftertreatment system, is a very

Fig. 8. Reactor product gas composition for  $\lambda = 3.25$ .

challenging task, as the requirements of reformat composition and reactor design are quite different.

On-board addition of water in the fuel reformer would increase further the H<sub>2</sub> production, but it will be rather impractical for conventional vehicles. However, alternative applications (such as off-road stationary engines), new powertrains (e.g. IC + fuel cell hybrids) and new fuels (e.g. stable hydrocarbon-water emulsions) may make it feasible to provide the reformer with higher feed-rates of water.

The O<sub>2</sub> and H<sub>2</sub>O contents of the exhaust gas of modern turbocharged diesel engines do not vary significantly between different engine load operating conditions or EGR additions as in the case of natural aspirated engines. For example, in natural aspirated engines the increase of the engine load or use of EGR results in considerable reduction of the O<sub>2</sub> availability in the exhaust. For this reason it will be easier to design a reformer and to control the reactants for a turbocharged diesel engine, since there is a significantly smaller range of engine exhaust gas compositions and conditions to be optimized. Furthermore, the design of an optimized fuel reformer for hydrocarbon-SCR is likely to reduce the need for post-engine fuel injection in other emission-control systems, such as particulate filters and NO<sub>x</sub> traps.

Finally, it has to be mentioned that although partial oxidation reformers are often considered for on-board applications due to their advantages in terms of quick start-up, fast response and compactness, their use for providing reformat to the particular hydrocarbon-SCR catalyst used in this study may be impractical because of their substantial CO production.

#### 4. Conclusions

As part of ongoing research towards the understanding and development of a diesel engine – exhaust gas fuel reformer – SCR system, an investigation of different reformer configurations and gas feed compositions has been carried out in order to meet the requirement of supplying the SCR 1%Pt/Al<sub>2</sub>O<sub>3</sub> catalyst with a reformat that will promote the catalyst low temperature NO<sub>x</sub> reduction. As has been shown in previous work, the reforming reactor design and operating parameters have to be such that the water gas shift reaction is an integral part of the reforming process. In addition, on-board a vehicle, the exhaust gas reformer will have to function over a vast range of engine exhaust gas compositions and space velocities.

The present experimental results have shown that the water gas shift reaction can be promoted by:

- Design of the reformer so that the intermediate reactants (i.e. the reactants just after the peak reactor temperature) will be kept for longer times in contact with the reforming catalyst cooler zones. This has been achieved by either increasing the length of the reforming catalyst bed or by dividing it into two parts. In the latter case, the second catalyst part has been placed at a location downstream of the first part where the reactor temperatures are lower (in the range of 500–700 °C) and thus the water gas shift reaction is favoured.

- Optimization of the quantity of the fuel supplied to the reformer according to the engine exhaust gas flows and compositions under different engine operating conditions. The reactant ratios have to be maintained at optimum values and, hence, flexible control of the fuel quantities supplied to the reformer is required.

#### Acknowledgments

The authors would like to thank Johnson Matthey Plc and Shell Global Solutions, UK for their support for this work.

#### References

- [1] A. Tsolakis, A. Megaritis, Catalytic exhaust gas fuel reforming for diesel engines – effects of water addition on hydrogen production and fuel conversion efficiency, *Int. J. Hydrogen Energy* 29 (2004) 1409.
- [2] A. Tsolakis, A. Megaritis, S.E. Golunski, Reaction profiles during exhaust-assisted reforming of diesel engine fuel, *Energy Fuels* 19 (2005) 744.
- [3] A. Tsolakis, A. Megaritis, Exhaust gas assisted reforming of rapeseed methyl ester for reduced exhaust emissions of CI engines, *Biomass Bioenergy* 27 (2004) 493.
- [4] A. Tsolakis, A. Megaritis, M.L. Wyszynski, Applications of the exhaust gas fuel reforming in compression ignition engines fuelled by diesel and biodiesel fuel mixtures, *Energy Fuels* 17 (2003) 1464.
- [5] A. Tsolakis, A. Megaritis, M.L. Wyszynski, Low temperature exhaust gas fuel reforming of diesel fuel, *Fuel* 83 (2004) 1837.
- [6] J. Naber, D. Siebers, Hydrogen combustion under diesel engine conditions, *Int. J. Hydrogen Energy* 23 (1998) 363.
- [7] A. Tsolakis, A. Megaritis, D. Yap, A. Abu-Jrai, Combustion characteristics and exhaust gas emissions of diesel engine supplied with Reformed EGR, SAE Paper No.: 2005-01-2087.
- [8] M. Kumar, A. Ramesh, B. Nagalingam, Use of hydrogen to enhance the performance of a vegetable oil fuelled compression ignition engine, *Int. J. Hydrogen Energy* 28 (2003) 1143.
- [9] A. Tsolakis, S. Golunski, Sensitivity of process efficiency to reaction routes in exhaust-fuel reforming of diesel fuel, *Chem. Eng. J.* 117 (2006) 131.
- [10] J. Kirwan, A. Quader, M. Grieve, Fast start-up on-board gasoline reformer for near-zero emissions in spark ignition engine, SAE Paper No.: 2002-01-101.
- [11] M.R. Salemi, J.R. Bennett, R.F. Nashburn, J. Kirwan, A.A. Quader, J.M. Haller, Method for starting a fast light-off catalytic fuel reformer, Patent No.: US 6,869,546 B2, Mar. 22, 2005.
- [12] R.F. Nashburn, M.R. Salemi, J. Kirwan, M.J. Grieve, Method and apparatus for rapid exhaust catalyst light-off, Patent Application No.: EP 1 522 697 A2, April 13, 2005.
- [13] B. Wen, NO reduction with H<sub>2</sub> in the presence of excess O<sub>2</sub> over Pd MFI catalyst, *Fuel* 81 (2002) 1841.
- [14] K. Yokota, M. Fukui, T. Tanaka, Catalytic removal of nitric oxide with hydrogen and carbon monoxide in the presence of excess oxygen, *Appl. Surf. Sci.* 121–122 (1997) 273.
- [15] R. Burch, M. Coleman, An investigation of the NO H<sub>2</sub> O<sub>2</sub> reaction on noble metal catalysts at low temperatures under lean-burn conditions, *Appl. Catal. B* 23 (1999) 115.
- [16] R. Burch, M. Coleman, An investigation of promoter effects in the reduction of NO by H<sub>2</sub> under lean-burn conditions, *J. Catal.* 208 (2002) 435.
- [17] B. Wichterlová, P. Sazama, J. Breen, R. Burch, C. Hill, L. Capek, Z. Sobalík, An in situ UV–vis and FTIR spectroscopy study of the effect of H<sub>2</sub> and CO during the selective catalytic reduction of nitrogen oxides over a silver alumina catalyst, *J. Catal.* 235 (2005) 195–200.
- [18] S. Satokawa, J. Shibata, K. Shimizu, A. Satsuma, T. Hattori, Promotion effect of H<sub>2</sub> on the low temperature activity of the selective reduction of NO by light hydrocarbons over Ag/Al<sub>2</sub>O<sub>3</sub>, *Appl. Catal. B* 42 (2003) 179.

- [19] M. Richter, U. Bentrup, R. Eckelt, M. Schneider, M. Pohl, R. Fricke, The effect of hydrogen on the selective catalytic reduction of NO in excess oxygen over Ag Al<sub>2</sub>O<sub>3</sub>, *Appl. Catal. B* 51 (2004) 261.
- [20] K. Eränen, F. Klingstedt, K. Arve, L. Lindfors, D. Murzin, On the mechanism of the selective catalytic reduction of NO with higher hydrocarbons over a silver/alumina catalyst, *J. Catal.* 227 (2004) 328.
- [21] A. Abu-Jrai, A. Tsolakis, The effect of H<sub>2</sub> and CO on the selective catalytic reduction of NO<sub>x</sub> under real diesel engine exhaust conditions over Pt/Al<sub>2</sub>O<sub>3</sub>, *Int. J. Hydrogen Energy* 32 (2007) 2073.
- [22] N. Macleod, R.M. Lambert, Lean NO<sub>x</sub> reduction with CO + H<sub>2</sub> mixtures over Pt/Al<sub>2</sub>O<sub>3</sub> and Pd/Al<sub>2</sub>O<sub>3</sub> catalysts, *Appl. Catal. B* 35 (2002) 269.
- [23] S. Peucheret, M. Feaviour, S. Golunski, Exhaust-gas reforming using precious metal catalysts, *Appl. Catal. B* 65 (2006) 201.
- [24] R. Horn, K.A. Williams, N.J. Degenstein, L.D. Schmidt, Syngas by partial oxidation of methane on rodium: mechanistic conclusions from spatially resolved measurements and numerical simulations, *J. Catal.* 242 (2006) 92.
- [25] R. Horn, N.J. Degenstein, A. Kenneth, K.A. Williams, L.D. Schmidt, Spatial and temporal profiles in millisecond partial oxidation processes, *Catal. Lett.* 110 (2006) 169.
- [26] R. Horn, K.A. Williams, N.J. Degenstein, L.D. Schmidt, Mechanism of H<sub>2</sub> and CO formation in the catalytic partial oxidation of CH<sub>4</sub> of Rh probed by steady-state spatial profiles and spatially resolved transients, *Chem. Eng. Sci.* 62 (2007) 1298.
- [27] J. Barbier, D. Duprez, Reactivity of steam in exhaust gas catalysis. I. Steam and oxygen/steam conversions of carbon monoxide and of propane over PtRh catalysts, *Appl. Catal. B* 3 (1993) 61.
- [28] B.I. Whittington, C.J. Jiang, D.L. Trimm, Vehicle exhaust catalysis. I. The relative importance of catalytic oxidation, steam reforming and water-gas shift reactions, *Catal. Today* 26 (1995) 41.